STUDY THE MICROHARDNESS AND SURFACE ROUGHNESS OF AS-BUILT AND HEAT-TREATED ADDITIVE MANUFACTURED IN718 ALLOY

Ajay Kumar MAURYA[1], Amit KUMAR[2]

Additive manufactured Inconel alloy produced by laser sintering technique can replace cast Inconel alloy in defense, automotive, and aerospace industries by offering more desirable mechanical and physical properties. This paper covers the building orientation and heat treatment effects on microhardness and surface roughness of additively fabricated IN718 alloy. Samples were built in three orientations (0^0, 45^0, 90^0) and subsequently heat-treated at 1080^0C/1 h (homogenization), 960^0C/1 h (solution treatment), and 720^0C/8 h (ageing). The Vickers hardness test and surface roughness test were performed before and after heat treatment. The results obtained from the tests were analyzed. A nearly 14.02% higher micro-hardness value (391.50 HV) was observed for 90^0 built samples heat-treated at 720^0C compared to 90^0 as-built samples, and nearly 13.62% lower surface roughness value (2.60 µm) was observed for 45^0 built samples heat-treated at 960^0C compared to 45^0 as-built samples.

Keywords: Additive manufacturing, Ni-Based Superalloy, DMLS, Heat-treatment, Micro-hardness, and Surface Roughness.

1. Introduction

Additive manufacturing (AM) is a layered process in which digital 3D design data is used to fabricate 3D parts by adding layer upon layer. In this process, a fine powder or wire-form raw material is used. The new creation technique permits specialists to plan complex parts that are hard to deliver using traditional strategies [1]. It is more practical since there is no material wastage as in regular assembling techniques [2]. It can deliver models of planned parts rapidly [3]. However, this new creation strategy needs to conquer a few difficulties like dimensional exactness, poor ductility, high surface roughness, and the formation of residual stress in the parts. The mechanical and physical properties like micro-hardness, density, strength, and creep of AM parts depend upon build orientation, heat-treatment, and process parameters [4].

[1] Research Scholar, National Institute of Technology Patna, India, e-mail: maurya.me16@nitp.ac.in
[2] Associate Professor, National Institute of Technology Patna, India. Email: amit@nitp.ac.in

Inconel 718 (IN718 alloy) is a highly demanded material in the industry for making, steam turbines for power plants, jet engines, and aircraft turbines due to its fine creep property, good fatigue strength, high yield resistance, and good weldability at higher temperatures. It is quite suitable for high-temperature applications up to 700 ^{0}C [5].

Various studies have focused on the effects of building orientation on the surface integrity and mechanical properties of AM parts. The mechanical characteristics of the structural bearing have varied because of anisotropy in the material. Several other research projects were focused on post-processing operations such as electropolishing [6], shot-peening [7], laser polishing [8], turning [9], heat-treatment [10], to improve the physical and mechanical properties of AM components. Tucho et al. [11] tested the hardness of SLM-printed IN718 before and after heat-treatment. The heat-treatment was performed at 1100 ^{0}C for 1 hour hold time. It was observed that the top and bottom regions of the sample exhibit a 13% difference in hardness due to heat treatment. Fayed et al. [12] investigated the effects of standard heat-treatment on the microstructure and mechanical properties of Inconel 718 components manufactured using additive manufacturing. After the heat-treatment process, the mechanical properties of AM components were considerably improved to the point where they were equivalent to those of wrought parts. Yusuf et al. [13] investigated the microstructural morphology of Inconel produced using a CO_2 laser beam and metal powders and demonstrated that the microstructure and laser beam scanning patterns were correlated. Furthermore, changes in the hardness were related to the ageing temperature difference. Donghyun et al. [14] fabricated Inconel 718 parts using wire arc additive manufacturing (WAAM) methods. Successive deposition resulted in an ageing effect that was observed in the deposition with cold metal transfer strengthening phases such as γ’ and γ″ were formed, which improved microhardness from 250 to 306 HV. The highest hardness value of each deposit was observed in the middle sections because of the high precipitation of these strengthening phases. The XRD analysis showed a reduced value of the lattice parameter, which indicated the formation of strengthening phases such as the γ″, γ′, and δ phases. Fayed et al. [15] investigated the effects of heat-treatment on AM fabricated Inconel 718 parts. They discovered a significant increase in hardness of nearly 51-72 percent when compared to the as-printed condition. This depends on the treatment period that developed γ′ and γ” in the γ-matrix when using the heat-treatment time frame. After 1 hour of homogenization, the hardest material was produced, but longer time treatments decreased the hardness. Lua et al. [16] have studied the deposited material characteristics in four different zones, i.e., the deposited layer, the transition zone, the heat-affected zone, and the base metal. The measured values for micro-hardness were 525 HV, 522 HV, 418 HV, and 302 HV respectively, indicating a progressive micro-hardness value depending on the measurement area.

The roughness on the top surface of the samples has been assessed in several studies in the literature [17-22]. These investigations give adequate process parameter information, and the majority of them show a similar pattern in which the roughness scales with the energy density applied to the surface. Spierings et al. [23], Yang et al. [24], Casalino et al. [25], and Bochuan et al. [26] all authors observed surface roughness decreases with energy density. However, as seen in literature, the influence of different building orientations and different heat-treatments on the micro-hardness and surface roughness of IN718 built by Direct Metal Laser Sintering (DMLS) has not been studied well yet.

In this study, the Inconel 718 samples produced by the DMLS method were subjected to different heat treatments. Micro-hardness and surface roughness were investigated and compared as a result of heat treatment.

2. Materials and methods

For the experiments, gas-atomized IN718 powder provided by EOS Germany was utilized. Approximately 15-40 µm powder particles were used. The microstructure and chemical composition of Inconel powder are shown in Fig. 1, and Table 1, respectively. As shown in Fig. 1, most of the powder particles have spherical shapes, but some of them have irregular shapes and sizes that contain pores and other small satellite particles attached to them.

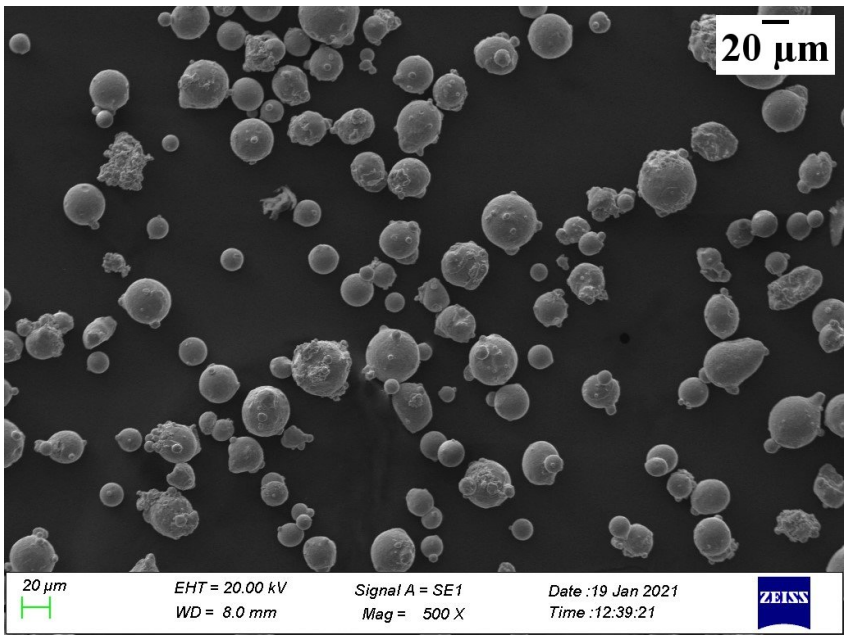

Fig. 1. SEM of as-received IN718 powder

Table 1

Elemental composition of Inconel 718

Element	Ni	Cr	Nb	Mo	Ti	*Al*	Co	Cu	C	B	Fe
Weight (%)	50-55	17-21	4.75-5.5	2.8-3.3	0.65-1.15	*0.2-0.8*	≤1	≤0.3	≤0.08	≤0.006	Balance

Studies were carried out to determine the influence of building orientation and heat-treatment on surface roughness and microhardness. Samples were fabricated on an EOSINT M280 L-PBF machine as shown in Fig. 2 (a) and the fabrication process is shown in Fig. 2 (b). In this process, metal powder is sintered using a laser as a power source to form an object layer by layer.

The build changer has a material dispensing platform and a building platform, as well as a coater blade used to move new powder across the build platform. In this process, a focused laser beam locally melts the metal powder and traces the cross-section of the object layer by layer to fuse the metal powder to the solid part. This means that you can develop very complex shapes. Before starting the fabrication process, the building substrate was preheated to 80 ^{0}C to minimize the thermal distortion in the sample.

In this paper, a set of cuboid specimens with a dimension of 10 mm x 35 mm x 5 mm is printed to investigate the hardness and surface roughness. All samples, as shown in Fig. 3, were fabricated in three building orientations (0^0, 45^0, 90^0) using the process parameters as given in Table 2. To create these parts, contouring was used, in which the laser travels around the part before the laser path creates a hatch shape within the part. (Bi-directional scan strategy was used). The manufacturing process is carried out in an argon atmosphere to protect the samples from oxidation.

Table 2

Process parameters are taken for building the samples

Parameter	Laser power	Layer thickness	Scan speed	Hatch spacing
Value	285 W	40 µm	960 mm/s	0.11 mm

Fig. 2. (a) DMLS setup

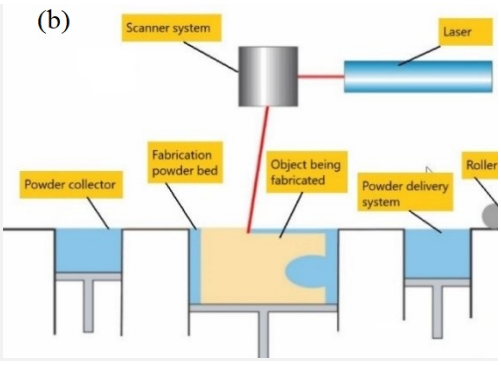

Fig. 2. (b) Showing fabrication process

The EOSINT-M280-DMLS AM system is used for sample fabrication. This equipment is available at the Central Tool Room and Training Center (CTTC), Bhubaneswar, India. The machine specification is: laser powder (400W), scan speed (7 m/s), wavelength (1060-1100 nm), laser type Yb-fiber laser, focused diameter of 100 µm, building volume 325 mm x 250 mm x 250 mm.

After the completion of the fabrication process, all samples were detached from the building substrate with the help of wire electro-discharge machining. A horizontal tube furnace is used to perform heat treatment as a post-process activity. The as-built (AB) samples are subjected to industry-standard heat treatment procedures that comply with the Aerospace Material Specification (AMS): HT1 (1080^0C/1h/FC (homogenization)), HT2 (960^0C/1h/FC (solution treatment)) & HT3 (720^0C/8h/AC (ageing)) Inconel 718 alloy [12]. HT1 as per the standard heat-treatment for cast IN718 (AMS 5383) and HT2 as per the standard heat-treatment for wrought IN718 (AMS 5662).

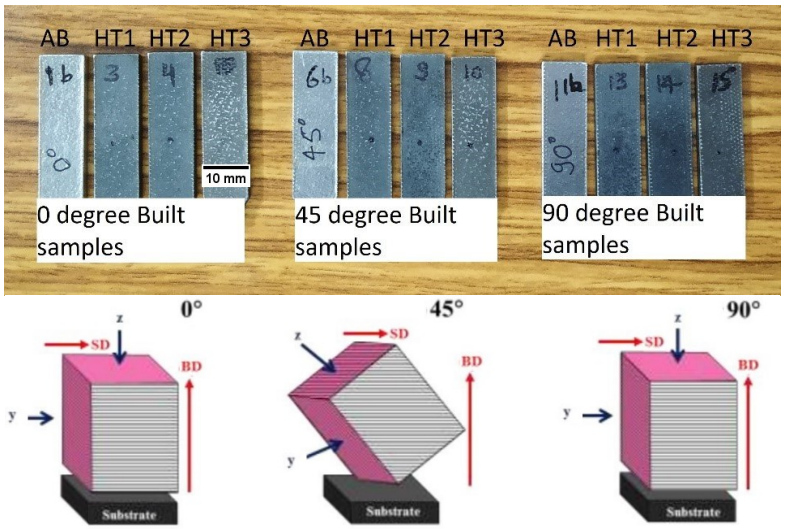

Fig. 3. Test samples used for testing and pictorial representation of 0^0, 45^0, and 90^0 deg. builds

All the fabricated and heat-treated samples were mechanically polished using silicon carbide paper, with a coarsening size ranging from 200 to 2500 followed by cloth cleaning. The microhardness measurement was carried out using a radial digital Vicker micro-hardness tester. For the hardness test, an indentation of a 1-kgf load was applied for a dwell period of 10 s. To acquire accurate results, at least ten uniformly distributed measurements were taken for each condition. All the measurements were made on the cuboid samples' xy-plane.

The surface roughness measurement was carried out on as-built and heat-treated samples using an optical profilometer. The surface roughness test was performed after as-built and heat-treatment without performing any surface

treatment process. To acquire accurate results, at least 10 observations were taken for each condition on the cuboid samples' xy-plane.

The phase was examined using X-ray diffraction (XRD) equipment. The test was performed at room temperature. Before starting the test, as-built and heat-treated samples were polished. Then, the polished samples are used for X-ray diffractometer measurements. Cu Kα radiation with a wavelength of 1.5406 Å was applied and measured in the range of 30-100^0 at intervals of 0.090 with an acquisition time of 2 s per increment.

The polished specimen was etched using an acid-based solution (HNO_3 (10 ml), acetic acid (10 ml), and HCl (15 ml)) to disclose the microstructure. The microstructural study was done using ZEISS scanning electron microscopy.

3. Results

3.1 Microhardness measurement

The microhardness variation of as-built and heat-treated samples was studied. The average microhardness values of as-built and heat-treated samples are shown in Fig. 4. Considering the 0^0, 45^0, and 90^0 as-built samples, the average microhardness values of 327.95, 337.61, and 343.34 HV were observed, respectively, and a higher micro-hardness value of 343.34 HV was observed for 90^0 as-built conditions. In cases of HT1, HT2, and HT3 conditions, the higher microhardness value of 391.50 HV was observed for the HT1 condition for 90^0 built samples, with an increase of 14.02% compared to 90^0 as-built samples. The improvement in micro-hardness under the HT1 condition is due to δ-phased precipitation hardening, which prevents dislocation motion. Increased microhardness at this heat treatment temperature is consistent with prior research [12, 27]. In the HT2 condition, the microhardness value was observed to be similar to the HT1 condition. These similarities in microhardness may be due to the nearly same heat-treatment condition for HT1 and HT2 samples, whereas in the case of the HT3 condition, the microhardness value decreases (23.30 %) to 300.25 HV for 90^0 built as compared to the 90^0 built HT1 condition and approximately 12.55% less compared to the 90^0 as-built conditions. The hardening observed in the HT1 and HT2 conditions appears as a softening in the HT3 condition. Residual stresses are one of the most prevalent issues that arise while using additive manufacturing. In the specimen's structure, residual stresses improve the specimen's microhardness. Performing a high-temperature heat treatment (say, > 900 ^{0}C) lowers residual stresses in the specimen, resulting in a microhardness decrease [33]. Performing the HT3 reduces microhardness because residual stresses have been eliminated from the specimen. According to another theory, high heat treatment temperatures (>900 ^{0}C) may dissolve the γ' and γ'' strengthening phases, (which might happen through the manufacturing process), resulting in a drop in microhardness [27].

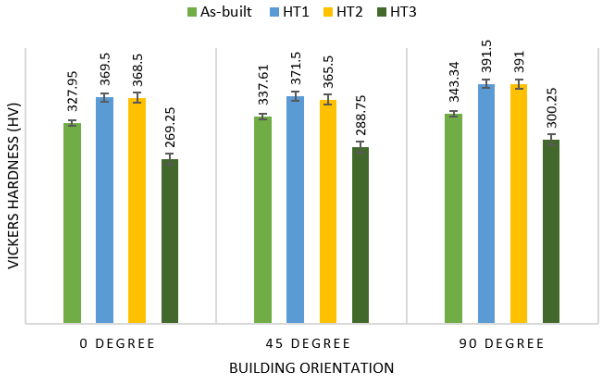

Fig. 4. Average micro-hardness value (HV) for as-built and heat-treated samples

3.2 Surface Roughness measurement

The average surface roughness is plotted against the building orientation. As shown in Fig. 5, the higher roughness value (Ra) of 4.24 µm was observed for 0^0 as-built samples, whereas the lower Ra value of 2.6 µm was observed for the 45^0 built HT1 condition. Compared among build orientations for as-built conditions, 45^0 built samples observed a 3.01 µm roughness value, which is nearly 29% lower than 0^0 as-built samples. As it was observed from Fig. 5, performing the HT1, HT2, and HT3 on samples reduces some amount of surface roughness compared to as-built samples for all orientations, respectively, but the surface roughness does not vary much among the HT1, HT2, and HT3 conditions, and they are nearly the same for all orientations, respectively.

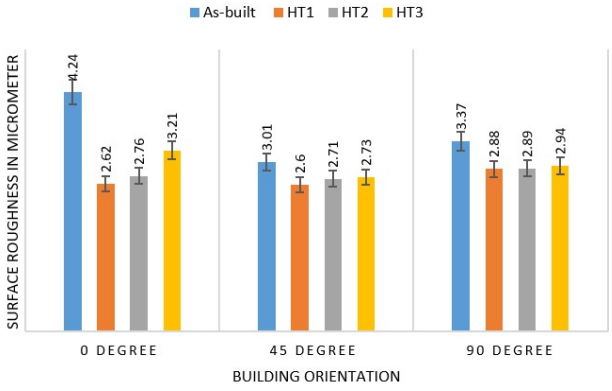

Fig. 5. Average surface roughness in µm was plotted for all conditions.

The reason behind the varying roughness is due to the remelting of pre-deposited layers that occurs in changing the specific area of heat flow in the case of as-built samples, and roughness decreases with energy density. Higher energy densities are attributed to material vaporization as well as increased porosity. Pores and un-

melted powder present on the surface play an important role in roughness. While performing the heat treatment, some of the pores are minimized and un-melted powder particles present on surfaces are refined to improve the surface roughness [34].

4. Discussion

4.1 Effect of the building orientation

The variation in the micro-hardness value is due to the thermal history changes between the layers during fabrication, and due to the building orientation, the interlayer time intervals lead to the changes in solidification time. Because of the remelting of pre-solidified layers, variation in specific regions of heat flow occurs, which was maximum in the case of 90^0 as-built samples. The solidification time changes during the remelting of the pre-deposited layer. An increase in solidification time means finer grains develop toward the building orientation that increases the microhardness. So, 90^0 as-built samples observed a higher micro-hardness value. As reported in the literature [28], orientation, anisotropy, and heat-treatment affect properties like micro-hardness.

As observed in Fig. 5, the surface roughness of samples produced by DMLS varies with build orientation. Horizontal (0^0) as-built surfaces presented a higher value of roughness, with an average Ra 4.24 μm, while perpendicular (90^0) as-built surfaces had an average Ra of 3.37 μm. The high-power laser beam melts the powder layer and partially melts the pre-solidified layers. A thermal gradient exists between the layers in the powder bed fusion process. This creates a high level of heat dissipation in the direction of the building. During the remelting of a pre-deposited layer, the influence of processing angle on the particular region of heat flow varies, causing surface roughness changes due to different solidification times between the layers [29]. The solidification time increased between the layers due to this fine grain being developed along the heat dissipation direction and along the building direction. The minimum surface roughness was observed. The higher roughness was observed for 0^0 as-built samples due to the large scan duration that results in a high volume of heat flow in pre-solidified layers, as also mentioned in literature [30].

4.2 Effect of heat treatment

Fig. 6 (a-i) shows the micrographs of heat-treated samples. The fine structure was seen when the sample was heat-treated (HT1, HT2, and HT3). During different heat treatments, some amounts of γ″ precipitates are formed, and because of the different heat-treatment cycles, the distribution of Nb near the grain

boundaries changes. During the heat-treatment cycles, cooling rates have little effect on grain size.

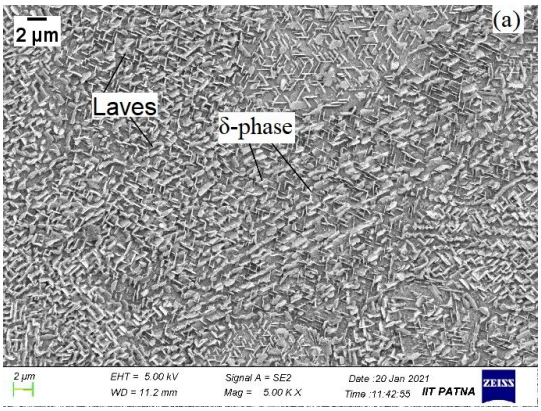

(a) 0 deg. build HT1

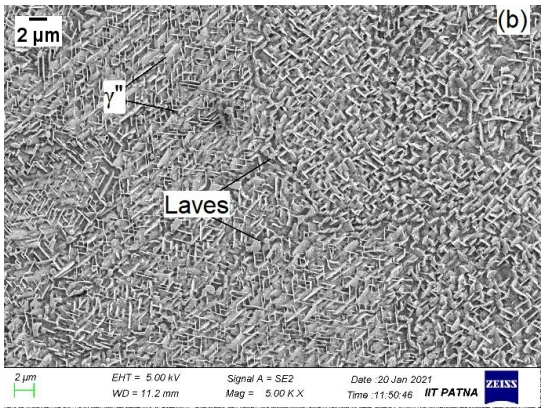

(b) 45 deg. build HT1

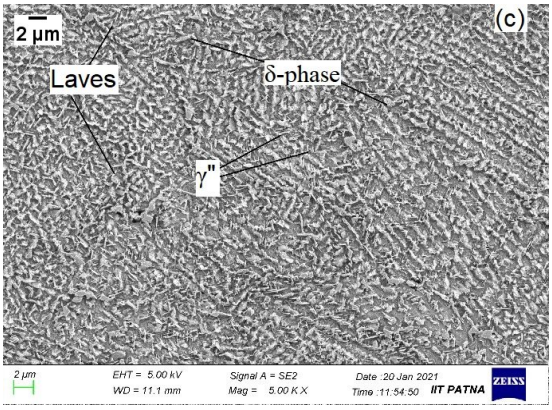

(c) 90 deg. build HT1

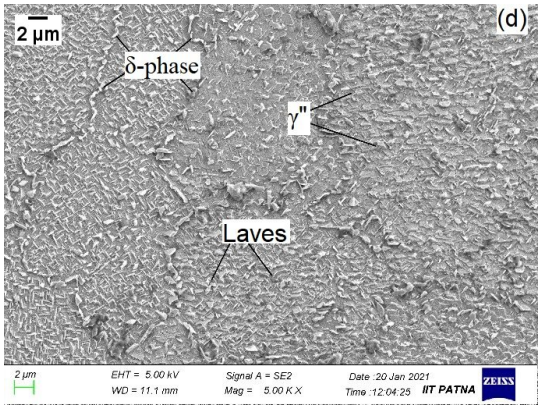

(d) 0 deg. build HT2

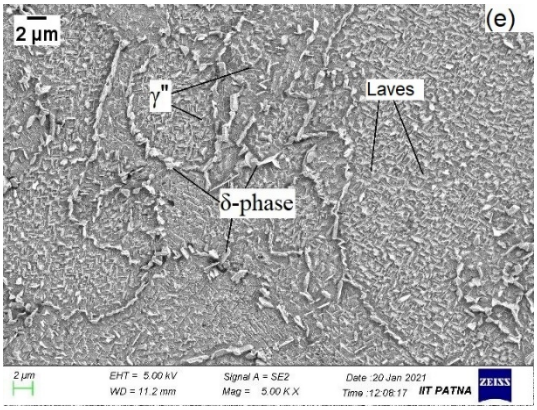

(e) 45 deg. build HT2

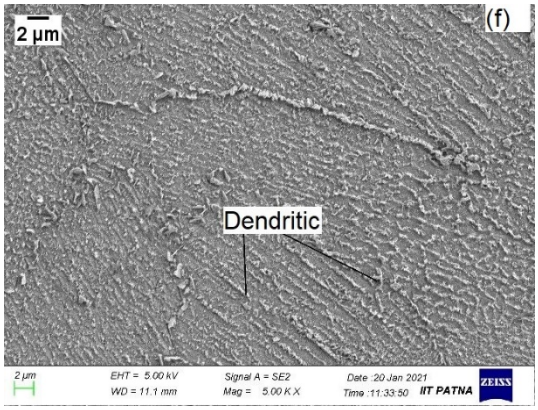

(f) 90 deg. build HT2

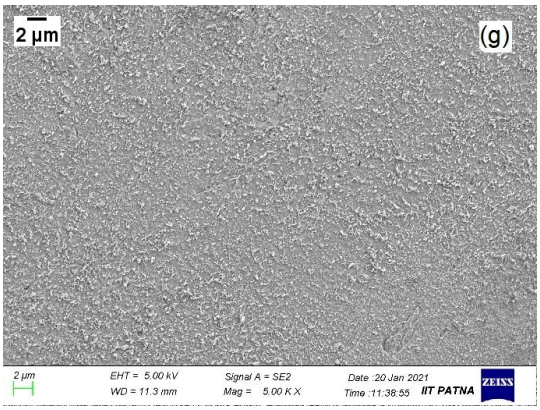

(g) 0 deg. build HT3

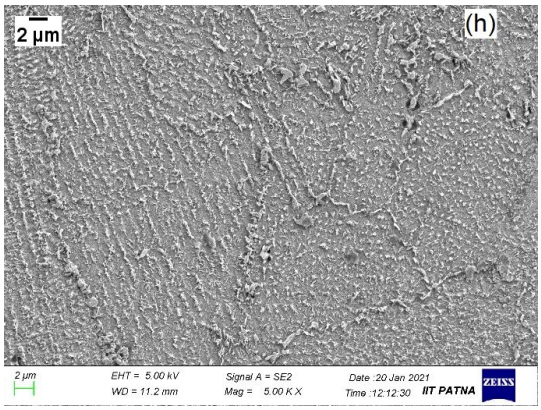

(h) 45 deg. build HT3

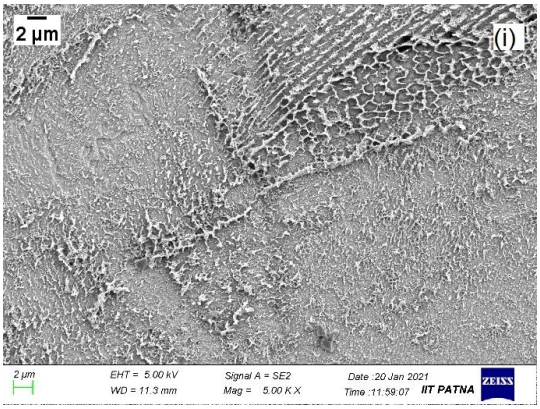

(i) 90 deg. build HT3

Fig. 6. SEM micrograph of heat-treated IN718 samples considering different building orientations.

The average micro-hardness value is shown in Fig. 4. The graph shows that the furnace-cooled HT1 and HT2 samples have relatively higher micro-hardness values than HT3 samples. An increase in micro-hardness value in HT1, and HT2 samples is due to precipitation of the strengthening phase such as the γ' and γ″ phases. It is a fine precipitate with the chemical composition of Ni_3(Al, Ti) that also serves as a strengthening phase. Also, δ-phase precipitates consume more Nb, which is a key alloying component for the γ" strengthening phase precipitation. As a result, δ-phase precipitation affects the mechanical properties of Inconel 718. The micro-hardness increases with the orientation that may be attributed to precipitates such as γ″ and γ' formed during heat-treatment because IN718 is a typical precipitation hardening alloy and strengthening is usually achieved through the post-heat treatment process [12]. In the XRD pattern, γ, δ, and NbC phases were indexed. According to Fig. 7, the rise in hardness values is due to the emergence of distinct strengthening phases, as demonstrated by the X-ray profiles of as-built, HT1, HT2, and HT3 samples.

4.3 XRD analysis

The XRD analysis was conducted for the test samples that had maximum hardness values, as illustrated in Fig. 7. It was observed from the phase analysis that the peak positions and peak intensities changed after applying various heat treatments. This means the evolution of microstructure in terms of texture and secondary phase dissolution and/or precipitation. The XRD pattern is drawn for the samples that have a case of maximum microhardness value. The peak was mainly attributed to the γ-matrix of the deposits. It is difficult to confirm the precipitation of the strengthening phase γ″ & γ' using XRD without prolonged annealing or coarsening of the precipitates. The strengthening phase, such as the γ″ and γ' dissolved in the γ-matrix that was partially formed and precipitated during deposition. It was observed that the peak intensity of (111) was lower than (200) in the case of HT3 samples compared to the powder, as-built, and HT1, and HT2 samples. It has been generally observed that the peak position changes with heat treatment and peak intensities that confirm textural and subsequent phase precipitation microstructural alterations. The lower peak intensity of γ (111) than of γ (200) suggests that performing HT3 for 2 h was not sufficient to modify the texture of the as-built sample along γ (200) as shown in Fig. 7.

After performing HT1, and HT2, a dissimilar XRD peak intensity was formed compared to the as-built sample. It was observed that the XRD patterns before and after heat treatment are similar in terms of texture, and there are no visible changes in the texture of the material that was also reported in the literature (Tucho et al.) [31]. During the heat treatments, the variations in peak locations demonstrate the precipitation and dissolution of Mo, Nb, and Ti [32]. γ (111) of the γ-matrix moved to higher diffraction angles after heat treatment due to the precipitation of the strengthening phases, γ" (Ni_3Nb), and γ' (Ni_3(Ti, Al)) that consumed Nb and Ti from the matrix. The distribution of precipitates such as γ', γ″ and δ revealed that the strengthening phase γ″ was larger in the sample HT1. The precipitation of the δ phase is also dependent on the residual strain and the amount of γ″ precipitates formed. The strengthening phase in the microstructure and XRD patterns confirmed the hardness findings.

Performing the heat treatment reduces the pore size and refines the surface texture, which improves some amount of surface quality. However, comparing the HT1, HT2, and HT3 conditions, it does not observe any significant changes among them in the surface roughness. Several changes were observed as a result of the change in the specific area of heat flow for remelting the solidified layers and the pores accessible at the surface.

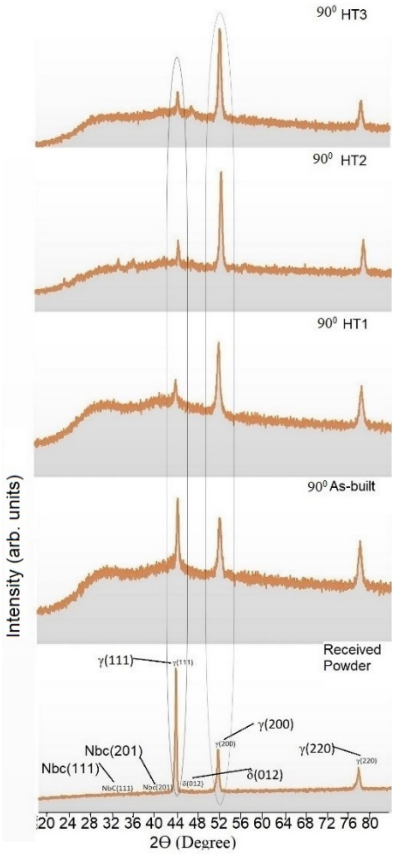

Fig. 7. An X-Ray diffraction pattern is drawn for the case of maximum microhardness value (Received powder, as-built, and heat-treated samples).

5. Conclusions

In this study, building orientation and heat treatment were examined for their effects on microhardness and surface roughness. The result obtained is given as follows.

- It was observed that the crystallographic orientation, precipitates, microstructure, and mechanical properties were all affected by homogenization treatment. The homogenization treatment performed at 1080 ^{0}C/1 h is insufficient to change the grain and texture structure of as-printed samples. Also, after this treatment, the laves phase and inter-dendritic segregates are only partially destroyed.
- It was observed that building orientation has a remarkable impact on hardness and roughness. Compared to horizontally and inclined built samples, vertically built samples have a greater stress concentration due to larger heat flow in the low specific area for laser melted regions that lead to deviations in hardness and

surface properties and also due to uneven localized melting and varying rates of heating-and-cooling and localized melting during sample fabrication.

- It was observed that a nearly 14.02% higher micro-hardness value (391.50 HV) for 90^0 built samples heat-treated at 720 ^{0}C compared to 90^0 as-built samples, and nearly 13.62% lower surface roughness value (2.60 μm) for 45^0 built 960 ^{0}C heat-treated samples compared to 45^0 as-built samples.
- The XRD analysis showed a reduced value of the lattice parameter, which indicated the formation of strengthening phases such as the γ', γ″, and δ phases that were also seen during SEM analysis.
- Higher temperature heat treatment (HT3) lowers residual stresses in the samples considerably, resulting in a decrease in microhardness due to the higher temperature. Some of the γ' and γ'' strengthening phases dissolve, resulting in a drop in microhardness.

Acknowledgment

I gratefully acknowledged that samples were fabricated at CTTC, Bhubaneswar. HT was done at NIT Patna and BIT Patna. Surface roughness, hardness, and microstructure were done at IIT Patna, and SEM and XRD were done at AKU Patna and were financially helped by the ministry of education.

REFERENCES

[1] *J.D. Herzog, and C. Emmelmann*, "Design guidelines for laser additive manufacturing of lightweight structures in TiAl6V4", Journal of Laser Applications, 2015, 27(S1), S14001.

[2] *B. Zhang, L. Dembinski, and C. Coddet*, "The study of the laser parameters and environment variables effect on mechanical properties of high compact parts elaborated by selective laser melting 316L powder", Materials Science and Engineering: A, 2013, 584, 21-31.

[3] *J.P. Kruth, M.C. Leu, and T. Nakagawa*, "Progress in additive manufacturing and rapid prototyping", Cirp Annals, 1998, 47(2), 525-540.

[4] *D. Bhaduri et al.,* "Laser polishing of 3D printed mesoscale components. Applied Surface Science", 2017, 405, 29-46.

[5] *M.J. Donachie, and S.J. Donachie*, "Superalloys: a technical guide", ASM international, 2002.

[6] U.S. Kim, and J.W. Park, "High-Quality Surface Finishing of Industrial Three-dimensional Metal Additive Manufacturing Using Electrochemical Polishing", International Journal of Precision Engineering and Manufacturing-Green Technology, 2019, 6 11-21.

[7] *B. AlMangour, and J.M. Yang*, "Improving the surface quality and mechanical properties by shot-peening of 17-4 stainless steel fabricated by additive manufacturing", Materials & Design, 2016, 110, 914-924.

[8] *F. Zhihao et al.,* "Laser Polishing of Additive Manufactured Superalloy" Procedia CIRP, 2018, 71, 150-154.

[9] *H. Yu et al.,* "Fatigue performances of selective laser melted Ti-6Al-4V alloy: Influence of surface finishing, hot isostatic pressing and heat treatments", International Journal of Fatigue, 2019, 120, 175-183.

[10] *K. Amato et al.,* "Microstructures and mechanical behavior of Inconel 718 fabricated by selective laser melting", Acta Materialia, 2012, 60(5), 2229-2239.

[11] *W. M. Tucho, P. Cuvillier, Atle Sjolyst-Kverneland, Vidar Hansen*, "Microstructure and hardness studies of Inconel 718 manufactured by selective laser melting before and after solution heat treatment", Materials Science and Engineering: A, 689, 2017, 220-232.

[12] *E. M. Fayed et al.,* "Influence of Homogenization and Solution Treatments Time on the Microstructure and Hardness of Inconel 718 fabricated by Laser Powder Bed Fusion", Materials, 2020, 1-23.

[13] *K. Yusuf, E. Tasciogu, Y. Kayanak*, "Heat treatment temperature-induced microstructure, microhardness and wear resistance of Inconel 718 produced by selective laser melting additive manufacturing", Optik, 2021, 227, (2021), 63907.
[14] *V. Donghyun, G.P. Dinda, P. Jaewoong, J. Mazumder, S.H. Lee*, "Enhancing hardness of Inconel 718 deposits using the aging effects of cold metal transfer-based additive manufacturing", Materials Science and Engineering: A, 776, 2020.
[15] *E.M. Fayed, M. Saadati, D. Shahriari, et al*. "Effect of homogenization and solution treatments time on the elevated-temperature mechanical behavior of Inconel 718 fabricated by laser powder bed fusion", Sci Rep 11, 2020.
[16] *X. Lua, Y.F. Zhou, X.L. Xing, B. Wang, Q.X. Yang, S.Y. Gao*, "Surface additive manufacturing of Ni-based superalloy/H13 steel system by laser depositing: Microstructure, microhardness and flexural response", Surface & Coatings Technology, 2018, 337, 525-535.
[17] *A.K. Maurya, A. Kumar*, "The Impact of Building Orientation on Microhardness & Surface Roughness of Direct Metal Laser Sintering Inconel Alloy", Advances in Mechanical Engineering. Lecture Notes in Mechanical Engineering. Springer, Singapore. (2021), 619-628.
[18] *F. Calignano, D. Manfredi, E.P. Ambrosio, L. Iuliano, and P. Fino*, "Influence of Process Parameters on Surface Roughness of Aluminum Parts Produced by DMLS," Int. J. Adv. Manuf. Technol., 2013, 67(9-12), 2743–2751.
[19] *K. Mumtaz, and N. Hopkinson*, "Top Surface and Side Roughness of Inconel 625 Parts Processed Using Selective Laser Melting," Rapid Prototyp. J., 2009, 15(2), 96-103.
[20] *M. Hamidi, D. Gastaldi, N. Francesca, and M. Vedani*, "On Morphological Surface Features of the Parts Printed by Selective Laser Melting (SLM)," Addit. Manuf., 24(October 2018), 373-377.
[21] *I. Yadroitsev, and I. Smurov*, "Surface Morphology in Selective Laser Melting of Metal Powders," 2011, 12, 264-270.
[22] *M. Yakout, A. Cadamuro, M.A. Elbestawi, and S.C. Veldhuis*, "The Selection of Process Parameters in Additive Manufacturing for Aerospace Alloys," 2017, 92, 2081-2098.
[23] *A. B. Spierings, N. Herres, G. Levy*, "Influence of the Particle Size Distribution on Surface Quality and Mechanical Properties in AM Steel Parts," Rapid Prototyp. J., 2011, 17(3), 195-202.
[24] *T. Yang, T. Liu, W. Liao, E. Macdonald, H. Wei, and X. Chen*, "The Process Parameters on Vertical Surface Roughness of the AlSi10Mg Parts Fabricated by Selective Laser Melting," J. Mater. Process. Tech., 2009, 26(September 2018), 26-36.
[25] *G. Casalino, S.L. Campanelli, N. Contuzzi, and A.D. Ludovico*, "Experimental Investigation and Statistical Optimisation of the Selective Laser Melting Process of a Maraging Steel," Opt. Laser Technol., 2015, 65, 151-158.
[26] *L. Bochuan, Wildman, R. C. Tuck, I. Ashcroft*, "Investigation the Effect of Particle Size Distribution on Processing Parameters Optimisation in Selective Laser Melting Process," Proc of the Annual Int Solid Freeform Fabrication Symp, University of Texas at Austin, Austin, 2015, 227-238.
[27] *V. Popovich, et al.,* Impact of heat treatment on mechanical behaviour of Inconel 718 processed with tailored microstructure by selective laser melting. Materials & Design, 2017. 131, 12-22.
[28] *T. Bharadwaj, M. Shukla,* "Direct Metal Laser Sintering of Maraging Steel: Effect of Building Orientation on Surface Roughness and Microhardness", Materials Today: Proceedings 5, 2018, 20485-20491.
[29] *L. Ventola, F. Robotti, M. Dialameh, F. Calignano, D. Manfredi, E. Chiavazzo*, PietroAsinarPie, "Rough surfaces with enhanced heat transfer for electronics cooling by direct metal laser sintering", Int. J. Heat Mass Transfer, 2014, 75, 58-74.
[30] *J. Delgado, J. Ciurana, C.A. Rodríguez*, "Influence of process parameters on part quality and mechanical properties for DMLS and SLM with iron-based materials", Int J Adv Manuf Technol, 2012, 60, 601-610.
[31] *W.M. Tucho, V. Hansen*, "Characterization of SLM-fabricated Inconel 718 after solid solution and precipitation hardening heat treatments", J. Mater. Sci. 2018, 54, 823-839.
[32] *R, Jiang, A. Mostafaei, J. Pauza, C. Kantzos, A. Rollett*, "Varied heat treatments and properties of laser powder bed printed Inconel 718. Mater. Sci. Eng. A 2019, 755, 170-180.
[33] *F. Ozanan Neves et al*. "Influence of Heat-treatment on Residual Stress in Cold-Forged Parts", Hindawi Publishing Corporation, 2014, 658679.
[34] *J.C. Snyder et al*., "Understanding Laser Powder Bed Fusion Surface Roughness", ASME Journal of Manufacturing Science and Engineering, 2019.